

The strength of stainless steel fillet welds using GMAW

M. Fortan, A. Dejans, D. Debruyne & B. Rossi

KU Leuven, Belgium

Abstract

This paper describes 18 tensile tests performed on welded specimens made of 3 stainless steel grades: EN 1.4307 (304L) and EN 1.4404 (316L) austenitic grades and EN 1.4062 duplex grade. For each grade, 3 tests were carried out along the direction of the weld causing shear stresses (in the weld throat plane, parallel to the weld throat axis) and 3 tests along the transverse direction causing a combination of normal (perpendicular to the weld throat plane) and shear (in the weld throat plane, perpendicular to the weld throat axis) stresses. The digital image correlation (DIC) technique was used to measure the initial geometry of the welds accurately in order to calculate their corresponding design strength. DIC was also used during testing to measure the strain field around the welds. Based on the experiments, an assessment of the current design rules is made and a modification of the correlation factor β_w is proposed.

Keywords

Stainless steel welds, experimental study, DIC, correlation factor β_w .

1 Introduction

For almost a century, stainless steel is used in construction as cladding because it combines an excellent aesthetic appearance with a good corrosion resistance and an ease of maintenance. Famous examples are the Chrysler building and the empire state building in New York, where stainless steel has been used for the iconic roofs which are still in outstanding state with only limited maintenance [1], most of the time limited to rain washing. Recently, stainless steels, and more especially duplex grades, gained more and more popularity as load-bearing elements in the construction and transport sector because it combines favourable aesthetic aspects, good mechanical properties and corrosion resistance hence a long-life span with little maintenance. This led to an increasing use of this material in structural components for applications such as (pedestrian) bridges, with multiple examples such as the Cala Galdana bridge in Menorca, the Siena Bridge in Ruffolo or the Millenium Bridge in York [2].

The components included in these applications can be both open or closed sections. Most of the time, these sections are welded. Therefore, research on the weldability and the strength of welds made of these grades is essential. Various studies show that the weldability of stainless steel is good and that most grades can be welded with all commonly used welding processes, granted that specific guidelines are followed. For duplex welds, an important feature is the balance between austenite and ferrite in the weld metal and the heat affected zone (HAZ). This can be guaranteed by a heat input lying in a suitable range. However, research on the strength of stainless steel welds is still scarce, with only 46 experiments available in [3]. Welds are designed by comparing the Von Mises stress in the weld throat plane to the resistance. The latter is divided by a correlation factor β_w , smaller or equal to 1.0, taking into account the variety of carbon steel grades. Research on high strength steel [4] suggest that a correlation factor β_w smaller than 1.0 is applicable for S460 grade which has a comparable strength as the studied duplex stainless steel grades. This suggests that these grades could also benefit from a lower correlation factor. In this paper, the experimental results are expanded for both duplex and austenitic stainless steels and the current correlation factor in EN 1993-1-4 is reassessed [5].

2 Literature review

2.1 Design rules

For the design of welded connections, EN 1993-1-4 [5], which contains the supplementary rules for stainless steel constructions, refers to the design rules stated in EN 1993-1-8 [6] for carbon steel. The value for the correlation factor β_w should be taken as 1.0 for all stainless steel families, except if tests in accordance with chapter 7 of EN 1993-1-4 justify a lower value.

For the design of fillet welds, the directional method is used. This method, see equation 1, uses the Von Mises criterion and compares the equivalent stress with the design value of the nominal ultimate strength of the weakest component. Additionally the normal stress perpendicular to the weld throat plane is limited by equation 2.

$$\sqrt{\sigma_{\perp}^2 + 3(\tau_{\perp}^2 + \tau_{\parallel}^2)} \leq \frac{f_u}{\beta_w \gamma_{M2}} \quad (1)$$

$$\sigma_{\perp} \leq \frac{0.9 f_u}{\gamma_{M2}} \quad (2)$$

where:

- σ_{\perp} is the normal stress perpendicular to the weld throat plane;
- τ_{\perp} is the shear stress, in the weld throat plane, perpendicular to the weld throat axis;
- τ_{\parallel} is the shear stress, in the weld throat plane, parallel to the weld throat axis;
- f_u is the nominal ultimate strength of the weakest joined part;
- β_w is the correlation factor dependant on the used material;
- γ_{M2} is the safety factor for connections.

When the full throat thickness a can be guaranteed along the entire weld, the whole length of the weld is used in the design. However, for most welds this is not the case in the start and end zones, leading to a reduction of the length with two times the throat thickness. The effective throat thickness should be taken as the height of the inscribed triangle, measured from the weld root to the outside leg of the triangle. When a deeper penetration can be guaranteed and proven by tests, this extra penetration can be taken into account, as shown in Fig. 1.

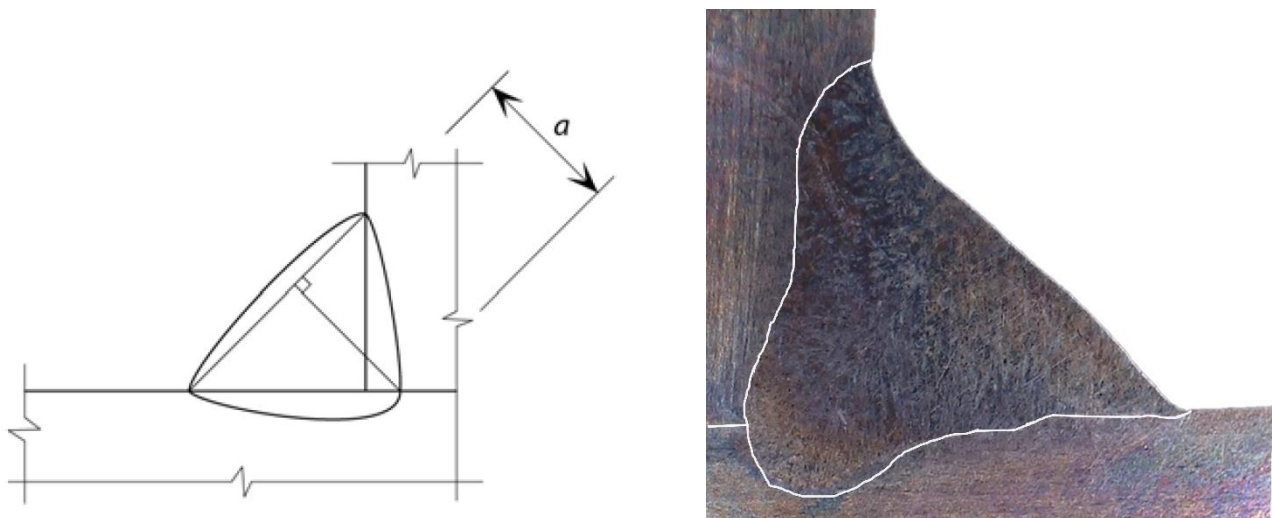


Fig. 1 Throat thickness a for a deep penetration fillet weld (left) and the macroscopic examination of the weld in EN 1.4062 (right).

2.2 Research on the strength of fillet welds

In the last decades, research on the strength of fillet welds has concentrated on high strength steel with different filler materials [4, 7-9]. Filler materials with a corresponding strength are difficult to find for very high strength steels and they have a limited ductility. Therefore, it is a common practise to undermatch filler materials for these grades to ensure the desired ductility of the joint. Besides the ductility, undermatching also influences the strength. EN 1993-1-12 [10] therefore uses the strength of the filler material in the strength function (equation 1 and 2) while most studies propose an average between the base and filler materials.

More importantly, Kuhlmann et al. [4,7] propose lowered correlation factors for high strength steels, including S460M which has a similar strength as the duplex stainless steels studied in this paper. The proposed factors depend on the steel grade but also on the load direction with a different correlation factor for butt welds, transverse fillet welds and longitudinal fillet welds. The study contains experiments on 328 specimens including several joint types and filler materials. The welds were welded in two phases. In the first phase a semi mechanized GMAW process was used, but, to reduce the scatter in the experimental results, in the second phase, a fully mechanized GMAW process was used, which resulted in more coherent test results. However, in practise, fully mechanized welding processes are not always available. The difference in strength for the transverse and longitudinal loading directions was confirmed in [11,12] and later for stainless steel in [3]. The fracture angles around 20° for the transverse welds in [11,12] are considerably lower than the theoretical critical angle of 45°, which could explain the higher strength.

The research on the strength of stainless steel fillet welds is quite limited with experiments published in [3,13] in contrast to the research on stainless steel weldability, which includes tensile tests and bending tests on butt welds, hardness measurements, impact tests and corrosion tests, see [14-23]. The tests performed by Errera et al. [13] included multiple loading directions and were conducted on the austenitic grade EN 1.4310, which is not included in table 2.1 of EN 1993-1-4 [5]. The report of Stangenberg [3] includes 23 tests on the austenitic grade EN 1.4301 and 23 tests on the duplex grade EN 1.4462 and all specimens were welded using a TIG-process. This process delivers a weld with a very high quality, but this quality comes at the expense of the productivity and therefore this process is rarely used in industrial practice. The experimental programme investigated both longitudinally and transversely loaded fillet welds and concluded that the correlation factor could be reduced for transverse welds but not for longitudinal welds.

3 Production of stainless steel fillet welds

3.1 Welding of stainless steel

Compared to mild steel, the welding of stainless steel comes with some additional difficulties. Complications can occur, depending on the grade and can be derived from the Schaeffler diagram shown in Fig. 2. This diagram consists of different zones related to the austenitic, ferritic and martensitic microstructures, according to the nickel and chromium equivalent entering the alloy composition. Depending on the location of an alloy in the diagram, its susceptibility to different problems can be assessed. Typically, martensitic steels are more vulnerable to hydrogen induced cracking due to their brittle microstructure. Ferritic stainless steels are more sensitive to grain growth since no phase changes, and thus no recrystallization, occur during heating. Those coarser grains are associated with inferior impact properties and lower strength. Austenitic stainless steels have a higher chance on solidification cracking, where high shrinkage strains in the weld pool and impurities cause a longitudinal fracture in the middle of the weld. For stainless steels with an austenite-ferrite structure (duplex stainless steels), a proper distribution between these two phases is important to guarantee optimal mechanical properties. Besides, they are susceptible for the occurrence of brittle intermetallic phases which also cause inferior mechanical and corrosion properties. Combining the location of the base material(s) and the filler material on the

Schaeffler diagram together with the dilution occurring during welding, gives the possibility to guarantee that the weld metal falls in the central region, where there are no complications.

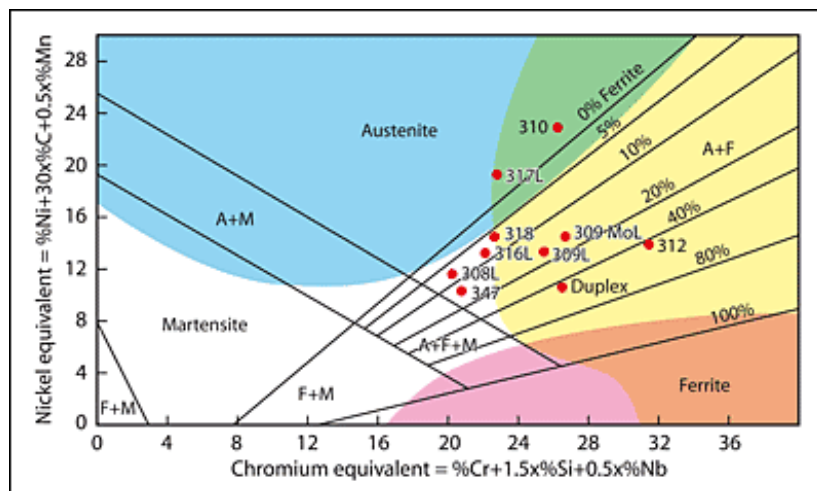


Fig. 2 Schaeffler diagram with location of commonly used alloys; A – austenite; F – ferrite; M – martensite; blue – hot cracking; yellow – sigma phase embrittlement;

In this study, alloys with an austenitic (EN 1.4307; EN 1.4404) and an austenitic-ferritic (EN 1.4062) microstructure are employed. For these materials, the following precautions should be taken.

Austenitic stainless steels

As mentioned, austenitic stainless steels are sensitive to solidification cracking. Impurities like phosphorus and sulphur have a detrimental influence on this phenomenon as they induce the occurrence of phases with a low melting point, causing a liquid film between the grains during solidification, which is not able to withstand the shrinkage forces. It is thus critical to use steels and filler materials with a low concentration of these impurities and to clean the workpieces before welding. The material certificates proved that the grades used in this study have low impurity concentrations. A microstructure containing a small amount of ferrite can help to reduce the influence because the impurities dissolve better in ferrite than in austenite. Besides, the ferrite grains increase the total amount of grain boundaries in the material so the low melting phases should cover a larger surface, not being able to form a continuous film. The austenitic materials used in this study inherently contain ferrite, as can be derived from the given Schaeffler diagram. An optimized geometry of the weld can also enhance the resistance to solidification cracking as welds with a high depth-to-width ratio are more prone to this type of failure. The reason can be found in the segregation of the low melting phases to the middle of the weld pool, where cracking will occur, rather than on the top of the weld. This can be considered during parameter selection and welding procedure optimisation. All welds in this research are single layer fillet welds, where the geometry is beneficial with respect to solidification cracking.

Duplex stainless steels

Because of the presence of ferrite in their microstructure, duplex stainless steels are less susceptible to solidification cracking. More importantly, the austenite-ferrite balance in the microstructure lies close to 50%-50% for the base material but can be heavily influenced by welding as rapid cooling, combined with the ferritic solidification, can prevent the formation of austenite. A low amount of austenite will result in a lower toughness and ductility, while an excessive amount of austenite would affect the strength and the resistance to stress corrosion cracking in a negative way. By controlling the heat input (and thus the welding parameters) in relation to the workpiece geometry and because of the added austenite forming elements in the filler material, the austenite content in the weld metal and the HAZ is guaranteed.

Besides the austenite-ferrite balance, duplex stainless steels are prone to the formation of sigma phase. This intermetallic phase causes brittle behaviour of the material and could be formed during reheating above 580°C. For this reason, one must be careful performing heat treatments, such as stress relieving, on duplex stainless steels. Apart from this, multi-layer welds can also cause the formation of sigma phase as the current pass heats up the previously welded layers. This can be prevented by using a maximum interpass temperature of 150°C. The tests performed in this study do not use any heat treatments or multi layered welds.

During welding, spatter and arc strikes on the base material should be prevented. These zones cause crevices where corrosion could occur or can, due to fast cooling, result in changes in microstructure with galvanic corrosion as a possible consequence. Weld spatter can be minimized by optimizing welding parameters and by welding in pulse arc regime, as done during this study.

3.2 Welding procedure and parameters

During this study, all welds were fillet welds produced using the gas metal arc welding (GMAW) process. This process has a high productivity, a high flexibility and can be used both manually and automatically, which makes it one of the most used processes in industry. To ensure a weld with sufficient penetration without using an excessively high heat input, welding was performed in pulse arc mode. Contrary to the short arc or spray arc modes, this transfer mode uses a pulsated current superimposed on a constant current. This way, the parameters are selected in such a way that an extra amount of energy is added at the moment a droplet of filler material is added to the weld. Hence no more energy than necessary is added to the weld and a lower heat input is maintained while guaranteeing a sound penetration.

The corresponding filler material for a stainless steel grade is chemically overmatched to ensure corrosion resistance but mechanically matched for structural integrity. For the tests performed during this study, the filler materials mentioned in Table 1 were used. For the EN 1.4307 grade, no corresponding filler material (type 304) exists. Typically, a type 308 filler material is used for welding this material but due to availability issues, a type 309 filler material was used instead. As the mechanical properties of both filler materials are similar, the conducted tests should not be influenced noticeably. However, type 309 and type 308 filler materials significantly differ in chemical composition (chromium and nickel content in particular), influencing the corrosion resistance of the weld zone.

The EN 1.4307 and EN 1.4404 grades were both welded with an argon-based shielding gas, supplemented with 2,5 % CO₂, while Arcal 129 gas was used for the EN 1.4062 material, which is an argon-based shielding gas with additions of nitrogen, CO₂ and helium.

The welding parameters were tested on pre-production test pieces, on which visual testing, microstructural investigation and hardness testing were performed. Different parameters were selected for the different materials, as summarized in Table 1.

The heat input, also mentioned in Table 1, was calculated from the measured voltage, current and travel speeds, combined with the efficiency factor for the gas metal arc welding process (80%). It is especially important when welding duplex stainless steels as it determines, together with factors as workpiece geometry or preheat temperature, the cooling rate and thus the austenite-ferrite balance of the material. For the used duplex grade, a heat input between 0,5 and 1,5 kJ/mm is recommended [24].

Table 1 Overview of welding parameters and resulting heat input.

Base material	Filler material	Travel speed	Wire speed	Voltage	Current	Pulse frequency	Heat input
		cm/min	m/min	V	A	Hz	kJ/mm
1.4307	type 309LSi	30	7,5	22,2	258	233	0,92
1.4404	type 316LSi	33	8,2	23	265	233	0,89
1.4062	Böhler CN 24/9 LDX	33	7,5	21	226	278	0,69

3.3 Quality assessment

Pre-production test pieces were subjected to visual inspection and the occurring imperfections were compared to the quality levels as mentioned in EN ISO 5817 [25]. The imperfections of the test pieces fell within the limits of quality level B, except intermittent undercut, which locally was inferior to quality level D.

The pre-production test pieces were cut, polished and etched for microstructural investigation. Test pieces of EN 1.4307 and EN 1.4404 were chemically etched with an acidified ferric chloride solution, while EN 1.4062 was electrolytically etched with a Lichtenegger and Bloech solution. Measuring the penetration of the weld was done using macroscopic investigation. As discussed before, microstructural investigation is particularly important for the EN 1.4062 samples, as the austenite-ferrite balance plays an important role concerning the mechanical and corrosion-related characteristics of the material. This balance was calculated based on microscopic images taken with a Hirox KH-8700 digital optical microscope at a magnification of 1000x. According to the description in ASTM E 562 [26], 30 images were analysed. Pixel counting was done by the ImageJ software [27]. The results of these tests are summarized in Table 2, together with the recommended values according to [28]. Apart from the base material, the measured zones lie in between, or close to, the limits of the recommended values.

Table 2 Measured and recommended ferrite contents for the EN 1.4062 material in different zones of the welded samples.

Zone	Measured ferrite content and 95% confidence interval (%)	Recommended ferrite content (%)
Base material	64 ± 8	40 to 60
Fusion zone	70 ± 8	25 to 75
Weld metal	61 ± 2	

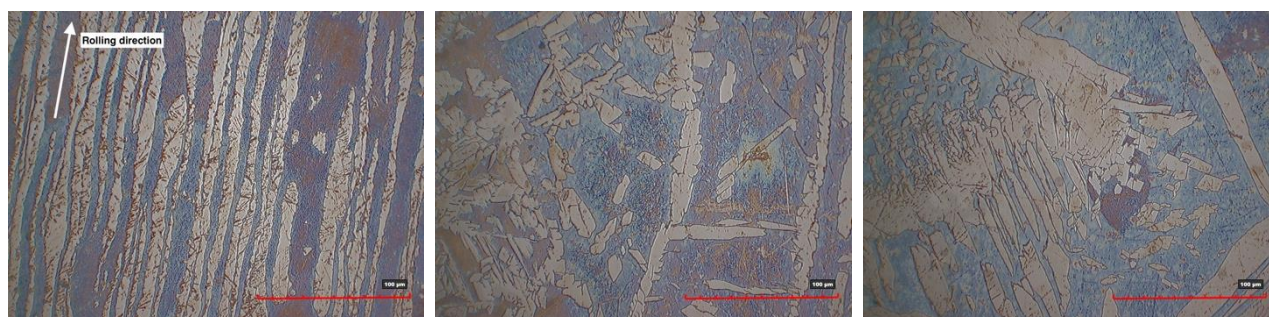


Fig. 3 Microstructure of EN 1.4062 samples: base material (left), fusion zone (middle) and weld metal (right). Ferrite matrix (blue) with austenitic zones (yellow).

On the same test pieces, Vickers hardness tests were performed. These tests were carried out in accordance with EN ISO 9015-1 [29], where a pattern, as shown in Fig. 4, was followed. No unexpected variation was visible from these measurements. By checking the location of the hardness measurements on the microscope, they could be divided between

base material and weld metal. Measurements in the fusion zone were not taken into account as the fusion zone was too small (no more than 0,15 mm) in comparison with the width of the indentations of the hardness measurements. Although the differences in hardness between the weld metal and base material may be statistically relevant in some cases, the values lie close to each other and no excessive differences in strength between those zones are expected. It should be noted that no assessment can be made for the strength of the fusion zone.

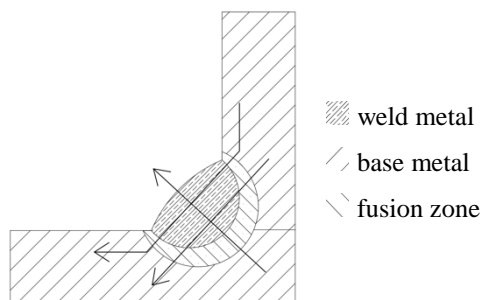


Fig. 4 Pattern used during Vickers hardness testing.

Table 3 Measured hardness values together with their 95% confidence interval.

Zone	Measured hardness with 95% confidence interval (HV5)		
	1.4307	1.4404	1.4062
Base material	187 ± 19	171 ± 14	257 ± 17
Weld metal	173 ± 15	179 ± 17	251 ± 11

4 Experimental program

This study, including a master thesis [30], concentrates on fillet welds welded using GMAW in two loading directions and three stainless steel grades, two austenitic grades EN 1.4307 (304L) and EN 1.4404 (316L) and one duplex grade EN 1.4062. Half of the tests were carried out with the load perpendicular to the welds causing both normal σ_{\perp} (perpendicular to the weld plane) and shear stresses τ_{\perp} (perpendicular to the weld throat axis) and the other half of the tests with the load parallel to the weld causing only shear stresses τ_{\parallel} (parallel to the weld throat axis). The initial geometry of the weld was measured using stereovision digital image correlation (DIC) and compared to the breaking surface after the test. During the test, all deformations were measured using DIC and post processed to obtain the average displacement between the plates. Stereo vision DIC is an optical measurement system that uses pictures taken by synchronized cameras of a speckle pattern on the specimens in the undeformed and deformed state. More information on this method can be found in [31] or more elaborate in [32].

4.1 Mechanical properties of the base material

One of the essential parameters in the current design rules is the strength of the weakest joined part. Herein, because no dissimilar joints were used, the ultimate strength of the base material should be used. In this study, it is chosen to disregard the effect of the filler material although, in the literature, it was proven that it can have an important influence. However filler materials having a limited overmatching strength were used, therefore the effect will be negligible. For the three stainless steel grades, three coupons cut in the same direction as the welded specimens were tested in tension. The two austenitic grades EN 1.4307 and EN 1.4404 exhibit a large ductility domain and significant strain hardening compared to the duplex grade EN 1.4062, which has a considerably higher yield strength combined with a smaller but still considerable ductility and strain hardening domains, as illustrated in Fig. 5.

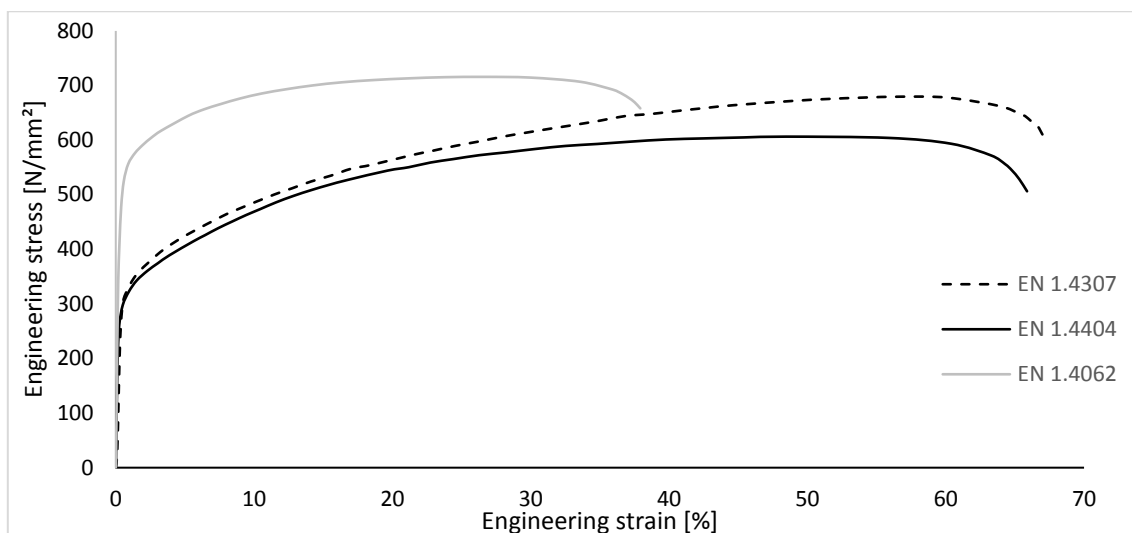


Fig. 5 Stress strain curve for EN 1.4307, EN 1.4404 and EN 1.4062

4.2 Experimental results

All tests were performed using a hydraulic tensile testing device with a maximum capacity of 1000 kN and the load was applied quasi statically with an average speed lower than 0.01 mm/s. The displacements were measured optically using two stereo vision DIC systems, one for the bottom welds and one for the top welds, both on only one side of the specimen. This system allows us to follow the displacement field of both plates and of the weld, before cracking. The load-displacement curves can be found in Fig. 6.

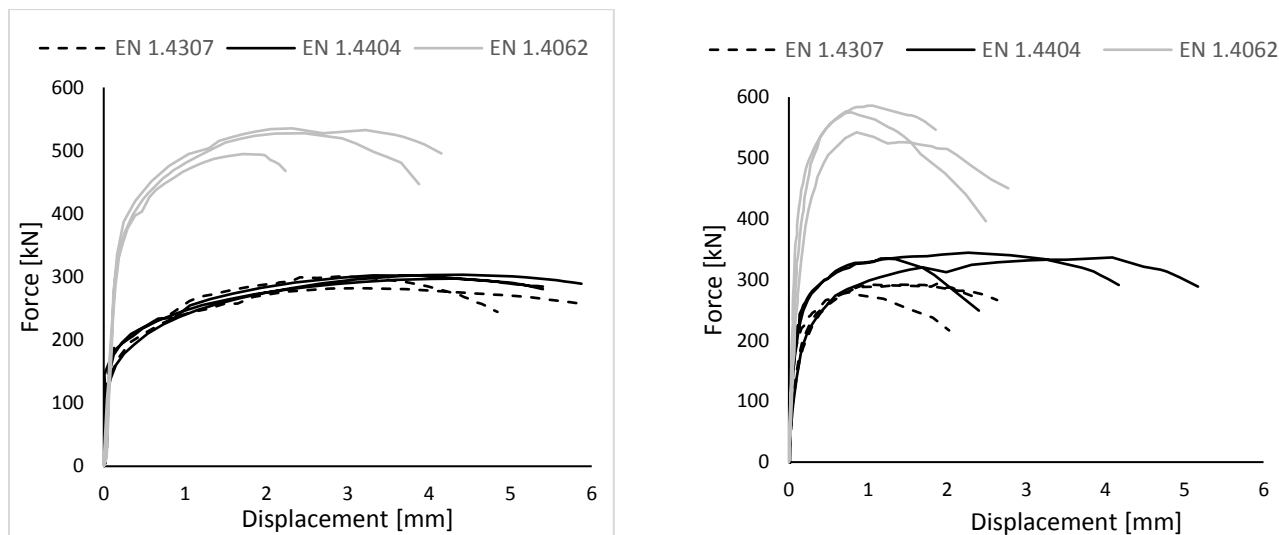


Fig. 6 Force-displacement curves of longitudinal welds (left) and transverse welds (right).

As can be seen in Fig. 6, the failure is ductile. All crack initiates in the start or end zone of the weld (in the end crater for most welds) and propagates until failure is reached. Typical failure modes can be seen in Fig. 7 for a longitudinal and a transverse weld. In general, the welds fail in the fusion zone at an angle ranging between 35° and 50° measured from the plate surface. Because the failure occurs in the weld metal, it can be concluded that the undercut, which is visible in some welds, doesn't have an influence on the ultimate loads. By measuring the weld throat over the whole length of the weld, the reduced area in the end zone is considered in the evaluation of the strength.



Fig. 7 Typical failure mode for longitudinal welds (left) and transverse welds (right).

4.3 Measurement of the weld surface

The area of the weld throat plane has a direct influence on the ultimate strength of the weld. Herein, multiple methods were used to evaluate this surface. First, the area is calculated using the nominal design values and the design rules in EN 1993-1-8 [6], as explained in section 2.1. However, in reality, the effective weld throat is larger than that, especially in the start and end zone where a divergence to this ideal value was noticed. It is therefore important to measure the weld throat surface over the whole length of the weld, which was presently done using DIC. By taking static pictures of the weld, MatchID [33], the software used for taking and post-processing the DIC pictures, generates a cloud of point of the outer surface of the weld as can be seen in Fig. 8. A post processing software, in this case CloudCompare [34], was used to calculate the actual throat thickness. The intersection of the surface of the bottom plate and of the side surface of the top plate was determined. From this line, the throat thickness a is measured at a 45° angle, which is the theoretically the critical plane. Multiple angles were measured, confirming that the 45° angle corresponds well with the minimal area.

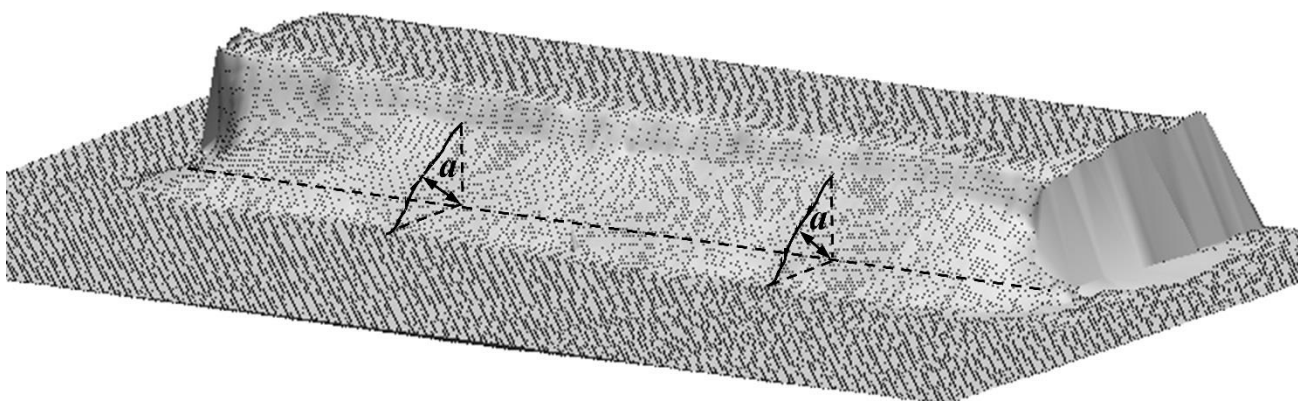


Fig. 8 3D point cloud of a measured weld with DIC.

Last, as EN 1993-1-8 [6] mentions, a deep penetration of the weld in the base material significantly increases the strength of the weld. In the macroscopic investigation, a large penetration was noticed up to 2.5 mm for the EN 1.4404 specimens. The measured throat thickness was hence enlarged along the effective length of the weld, i.e. along $l - 2a$ as described in 2.1 (in the start and end zones, inferior penetration occurs). The best, but most demanding method to assess the weld area is measuring the fracture area after the tests. The roughness of the fracture surface and the varying fracture angle along the weld length have to be taken into account. Analog to the measurements of the effective throat thickness, the fracture areas of the duplex specimens were measured using DIC.

5 Assessment of the design rules

The experimental ultimate loads were compared to the design rules in multiple ways, as can be seen in Table 4. For every assessment, the safety factor γ_{M2} is taken as 1. The first comparison is made using the nominal geometry of the specimens and the nominal ultimate strength of the base material, as would be utilized in a traditional design and is shown in equation 3. This comparison has a high average experimental-to-predicted strength ratio of 2.15 due to the difference between the designed throat thickness and the effective throat thickness. The start and end zones are considered by decreasing the weld length according to the rules in EN 1993-1-8 [6] for the design values, in contrast to the other methods where a measured weld throat length is used over the whole length. The second comparison, equation 4, uses the weld throat length a_{eff} at a 45° angle as determined using the DIC measurements before testing. This gives an accurate estimation of the weld throat length over the whole weld length. However, penetration in the base material is neglected, which results in an underestimation of the strength, with an average ratio of 1.41. The penetration i , which was measured in the macroscopic examination for every grade, is added in the third method (equation 5) along a reduced length of $l - 2a$, resulting in better predictions of the strengths. Last, taking into account the measured fracture surface for the duplex specimens in equation 6, the actual predicted strengths become approximately 10 % lower than equation 5. The penetration, which is not constant over the length of the weld due to manual welding, and the local imperfections in the weld explain this difference.

$$A_1 = a_{nom} * (l_{nom} - 2a_{nom}) \quad (3)$$

$$A_2 = a_{eff} * l_{eff} \quad (4)$$

$$A_3 = a_{eff} * l_{eff} + i * (l_{eff} - 2a_{eff}) \quad (5)$$

$$A_4 = A_{fracture} \quad (6)$$

where:

- A_i is the area used in equation 1 and 2 to determine the stresses for method i;
- a_{nom} is the nominal throat thickness;
- l_{nom} is the nominal length of the weld;
- a_{eff} is the effective throat thickness measured using DIC;
- l_{eff} is the effective length of the weld measured using DIC;
- i is the extra penetration measured using the macroscopic investigation;
- $A_{fracture}$ is the fracture area measured in 3D using DIC.

Table 4 Overview of test results

Name	Test	Design values		a through DIC measurement		Extra weld penetration		Fracture surface	
	F_{exp}	F_{pred}	F_{exp}/F_{pred}	F_{pred}	F_{exp}/F_{pred}	F_{pred}	F_{exp}/F_{pred}	F_{pred}	F_{exp}/F_{pred}
-	kN	kN	-	kN	-	kN	-	kN	-
14307L1	302	125	2.42	202	1.49	285	1.06		
14307L2	299	125	2.40	228	1.31	308	0.97		
14307L3	284	125	2.28	227	1.25	302	0.94		
14307T1	297	139	2.15	240	1.24	321	0.93		
14307T2	281	139	2.03	221	1.27	296	0.95		
14307T3	292	139	2.11	216	1.35	302	0.97		
14404L1	303	139	2.18	213	1.43	313	0.97		
14404L2	297	139	2.13	189	1.57	294	1.01		
14404L3	303	139	2.18	210	1.45	313	0.97		
14404T1	338	153	2.21	234	1.44	345	0.98		
14404T2	337	153	2.20	253	1.33	359	0.94		
14404T3	343	153	2.24	259	1.33	373	0.92		
14062L1	529	258	2.05	351	1.51	504	1.05	467	1.13
14062L2	495	258	1.92	325	1.52	478	1.04	423	1.17
14062L3	536	258	2.07	349	1.54	504	1.06	469	1.14
14062T1	576	279	2.06	422	1.37	570	1.01	505	1.14
14062T2	587	279	2.10	419	1.40	562	1.04	493	1.19
14062T3	543	279	1.94	362	1.50	505	1.07	505	1.07
		Average	2.15	Average	1.41	Average	0.99	Average	1.14
		Standard deviation	0.136	Standard deviation	0.104	Standard deviation	0.051	Standard deviation	0.040

6 Conclusions

Two factors have an important influence on the results: the ultimate strength of the weakest component and the weld throat plane. It is shown in the literature review on carbon steel fillet welds that mechanically overmatched or undermatched filler materials have a clear influence on the weld strength. In this study, matching filler materials were used. Besides, the influence of the weld throat surface was investigated through different ways of measurement. Using the effective weld throat length at 45° over the whole weld length together with the extra penetration weld along a reduced weld length of $l - 2a$ gives, on average, satisfactory results. However, if the fracture surface is measured in 3D, which was achieved in this study for the six duplex stainless steel specimens, it results in an actual area which is approximately 10% lower than this approximate value. For those specimens, an average experimental-to-predicted strength ratio of 1.14 is found (COV of 0.035), for both longitudinal and transverse welds, resulting in a correlation factor β_w of 0.88 (only for a population of 6 tests). For the austenitic stainless steel grades, the three other methods were used to assess the strength. A slightly lower strength compared to the duplex specimens was found, leading to the preliminary conclusion that a correlation factor of 1, as proposed in EN 1993-1-4 [5], is suitable for austenitic stainless steel grades. In [3], the same conclusions were drawn, with a slightly higher strength for the duplex specimens compared to the considered austenitic grades. However, in this report, a clear difference between longitudinal and transverse loaded welds was observed in contrast to the present observations. Other references [4,7,11,12] confirm the difference between the two loading directions. Some [11,12] state a fracture angle of about 20° although all specimens in this paper (both longitudinal and transverse) failed at an angle ranging between 35° and 50° . Further research is necessary to investigate the origin of these differences. Currently, a campaign of 30 additional tests using various welding procedures is ongoing. The additional results will enable us to conclude on the correlation factor for duplex and austenitic stainless steel.

7 Acknowledgements

The first author is funded by a PhD fellowship from the Research Foundation Flanders. We would also like to thank Industeel for granting the duplex material for this research.

References

- [1] International stainless steel forum, Stainless steel in architectural applications, 2016
- [2] Baddoo N.R., Kosmač A., Sustainable Duplex Stainless Steel Bridges, (www.wordstainless.org). 2010
- [3] Stangenberg, H. Final report. ECSC Project – Development of the use of stainless steel in construction, tech. Rep. RT810, contract No. 7210 SA/842. The steel construction institute, 2000.
- [4] Günther, H.P., Hildebrand, J., Rasche, C., Versch, C., Wudtke, I., Kuhlmann, U., Vormwald, M., Werner, F. Welded connections of high-strength steels for the building industry. *Welding in the world*, 56, 86-106, 2012.
- [5] European Committee for Standardization (CEN), Eurocode 3: design of steel structures - part 1-4: General rules - Supplementary rules for stainless steels. Brussel Cen, Brussel, 2015.
- [6] European Committee for Standardization (CEN), Eurocode 3: design of steel structures - part 1-8: Design of joints. Brussel Cen, Brussel, 2009.
- [7] Kuhlmann, U., Günther, H.-P., Rasche, C. High-strength steel fillet welded connections. *Steel Construction*, 1, 77-84, 2008.
- [8] Collin, P., Johansson, B. Design of welds in high strength steel. International conference on steel and composite structures. Maastricht, The Netherlands, 2005.
- [9] Khurshid, M., Barsoum, Z., Mumtaz, N.A. Ultimate strength and failure modes for fillet welds in high strength steels. *Materials and Design*, 40, 36-42, 2012.
- [10] European Committee for Standardization (CEN), Eurocode 3: design of steel structures - part 1-12: Additional rules for the extension of EN 1993 up to steel grades S 700. Brussel Cen, Brussel, 2009.
- [11] Björk, T., Toivonen, J., Nykänen, T. Capacity of fillet welded joints made of ultra high strength steel. Finland: Lappeenranta University of Technology, 2012.
- [12] Lu, H., Dong, P., Boppudi, S. Strength analysis of fillet welds under longitudinal and transverse shear conditions. *Marine structures*, 43, 87-106, 2015.
- [13] Errera, S.J., Tang, B.M., Popowich, D.W. Strength of bolted and welded connections in stainless steel, Report No. 335. Cornell University, Department of structural engineering, 1970.
- [14] Luo, J., Dong, Y., Li, L., Wang, X. Microstructure of 2205 duplex stainless steel joint in submerged arc welding by post heat treatment. *Journal of manufacturing process*, 16, 144-148, 2013.
- [15] Lakshminarayanan, A.K., Shanmugam, K., Balasubramanian, V. Effect of welding processes on tensile and impact properties, hardness and microstructure of AISI 409M ferritic stainless joints fabricated by duplex stainless steel filler metal. *Journal of iron and steel research, international* 16, 66-72, 2009.
- [16] Mohandas, T., Reddy, G.M., Naveed, M. A comparative evaluation of gas tungsten and shielded metal arc welds of a “ferritic” stainless steel. *Journal of materials processing technology*, 94, 133-140, 1998.
- [17] Asif, M.M., Shrikrishna, K.A., Sathiya, P., Goel, S. The impact of heat input on the strength, toughness, microhardness, microstructure and corrosion aspects of friction welded duplex stainless steel joints. *Journal of manufacturing processes*, 18, 92-106, 2014.
- [18] Rahmani, M., Eghlimi, A., Shamanian, M. Evaluation of microstructure and mechanical properties in dissimilar austenitic/super duplex stainless steel joint. *Journal of materials engineering and performance*, 23, 3745-3753, 2014.
- [19] Gotkowski, P., Jachym, R., Fryc, H. Duplex steel welding in the construction of railway vehicles. *Welding International*, 28 (12), 917-922, 2013.
- [20] Kumar, S., Shahi, A.S. Effect of heat input on the microstructure and mechanical properties of gas tungsten arc welded AISI 304 stainless steel joints. *Materials and design*, 32, 3617-3623, 2010.
- [21] Luo, J., Wang, X., Yao, Z. Double-sided single-pass submerged arc welding for 2205 duplex stainless steel. *Journal of materials engineering and performance*, 22 (9), 2477-2486, 2012.
- [22] Ohata, M., Namekata, T., Satoh, S., Okazaki, T., Shimura, Y., Watanabe, H. Load-carrying capacity of overmatched welded joint of stainless steel for building structure. *Weld world*, (28), 743-753, 2012.

- [23] Westin, E.M. Microstructure and properties of welds in the lean duplex stainless steel LDX 2101®. Doctoral thesis Royal Institute of Technology Stockholm, 2010.
- [24] Kotecki, D.J. Some Pitfalls in Welding of Duplex Stainless Steels. *Soldagem & Inspeção*, 15 (4), 336-343, 2010.
- [25] ISO 5817, Welding - Fusion-welded joints in steel, nickel, titanium and their alloys (beam welding excluded) - Quality levels for imperfections. Standard, International Organisation for Standardisation, Geneva, CH, 2014.
- [26] ASTM E562-11, Standard Test Method for Determining Volume Fraction by Systematic Manual Point Count, ASTM International, West Conshohocken, PA, 2011.
- [27] ImageJ (version 2) [GPL software]. Retrieved from <http://www.imagej.net/>. 2017
- [28] Van Nassau, L., Meelker, H., Hilkes, J. Welding duplex and super-duplex stainless steels. *Duplex Stainless Steels'91*. 1 303-323, 1991.
- [29] ISO 9015-1, Destructive tests on welds in metallic materials - Hardness testing - Part 1: Hardness test on arc welded joints, Standard, International Organisation for Standardisation, Geneva, CH, 2011.
- [30] Maes, A., Mertens, S. Experimental study of the strength of austenitic and duplex welds. Master thesis, KU Leuven campus De Nayer, 2017
- [31] Fortan, M., De Wilder, K., Debruyne, D., Rossi, B. Shear buckling of lean duplex stainless steel plate girders with non-rigid end posts. *Proceedings of the 8th International Conference on Steel and Aluminium Structures 2016*. Hong Kong, China. 2016.
- [32] Sutton, M. A., Ortu, J.-J., Schreier, H. W. *Image Correlation for Shape, Motion and Deformation Measurements: Basic Concepts, Theory and Applications*. 2009.
- [33] MatchID, www.matchidmbc.be
- [34] CloudCompare (version 2.8.1) [GPL software]. Retrieved from <http://www.CloudCompare.org/>. 2017